A comprehensive analysis of protein–protein interactions in *Saccharomyces cerevisiae*

Peter Uetz*†, Loic Giot*‡, Gerard Cagney†, Traci A. Mansfield‡, Richard S. Judson‡, James R. Knight‡, Daniel Lockshon†, Vaibhav Narayan‡, Maithreyan Srinivasan‡, Pascale Pochart‡, Alia Qureshi-Emili†§, Ying Li‡, Brian Godwin‡, Diana Conover†§, Theodore Kalbfleisch‡, Govindan Vijayadamodar‡, Meijia Yang‡, Mark Johnston†‖, Stanley Fields†§ & Jonathan M. Rothberg‡

‡ *CuraGen Corporation, 555 Long Wharf Drive, 11th Floor, New Haven, Connecticut 06511, USA*
† *Departments of Genetics and Medicine and § Howard Hughes Medical Institute, University of Washington, Box 357360, Seattle, Washington 98195-7360, USA*
* *These authors contributed equally to this work*

Two large-scale yeast two-hybrid screens were undertaken to identify protein–protein interactions between full-length open reading frames predicted from the *Saccharomyces cerevisiae* genome sequence. In one approach, we constructed a protein array of about 6,000 yeast transformants, with each transformant expressing one of the open reading frames as a fusion to an activation domain. This array was screened by a simple and automated procedure for 192 yeast proteins, with positive responses identified by their positions in the array. In a second approach, we pooled cells expressing one of about 6,000 activation domain fusions to generate a library. We used a high-throughput screening procedure to screen nearly all of the 6,000 predicted yeast proteins, expressed as Gal4 DNA-binding domain fusion proteins, against the library, and characterized positives by sequence analysis. These approaches resulted in the detection of 957 putative interactions involving 1,004 *S. cerevisiae* proteins. These data reveal interactions that place functionally unclassified proteins in a biological context, interactions between proteins involved in the same biological function, and interactions that link biological functions together into larger cellular processes. The results of these screens are shown here.

With the completion of the genome sequence of the budding yeast *Saccharomyces cerevisiae* in April 1996 (ref. 1), a eukaryotic organism could be analysed on a genomic scale for the first time. The challenge became one of understanding the roles of the approximately 6,000 gene products and how they interact to create a eukaryotic organism. However, one-third of the predicted yeast open reading frames (ORFs) are still classified as proteins of unknown function[2]. Genomic technologies have been developed that focus predominantly on the use of DNA array approaches to measure, for example, the expression of large sets of genes. As comparable strategies for protein analysis are not available, we initiated two types of systematic study to produce additional information that can place yeast ORFs within a biological context, with the goal of understanding their functional roles. We chose to use the yeast two-hybrid system because it can identify pairs of proteins that physically associate with one another[3] and because two-hybrid screens are simple, sensitive and amenable to high-throughput methods. The first genomic analysis using the two-hybrid system centred on the T7 bacteriophage[4]. Large complexes in *S. cerevisiae* have also been analysed using this method of detecting protein–protein interactions[5,6]. Here we present the results of two complementary strategies using the two-hybrid screen to identify protein–protein interactions among the predicted ORFs of *S. cerevisiae*. A bioinformatics platform for the analysis of this data set is publicly available at http://portal.curagen.com.

A protein array of activation-domain hybrids

To examine protein activity in a format that allows the assay of every predicted ORF, we constructed an array of hybrid proteins. At least two general types of protein array may be envisioned: those composed of living transformants, as described here, with each protein expressed in a form that allows expedient assay of the host cells; and those composed solely of the purified proteins[7]. The two-hybrid array used here is a set of yeast colonies derived from about 6,000 individual transformants. The transformation event inserts one of the yeast ORFs into a Gal4 transcription-activation domain vector to create a hybrid protein. To enable rapid, large-scale transformation, we generated those ORFs as a set of polymerase chain reaction (PCR) products with 70 base-pair sequences at their 5′ and 3′ ends that precisely matched sequences in the activation domain vector pOAD[8]. These sequences allowed highly efficient recombination between the ORFs and the linearized vector. After transformation of a yeast two-hybrid reporter strain[9], we pooled two colonies from each transformation plate to constitute a single array element (Fig. 1a), with the entire array contained on sixteen microassay plates of 384 colonies each.

A set of 192 DNA-binding domain hybrids was similarly generated by transformation into a strain of opposite mating type of PCR products with a Gal4 DNA-binding domain vector. To screen for protein interactions, we mated a transformant containing one of the DNA-binding domain hybrids to all of the transformants of the array, selecting diploids using markers carried on the two-hybrid plasmids. The diploids were then transferred to selective plates deficient in histidine, and colonies positive for the two-hybrid reporter *HIS3* gene were identified by their positions in the array (Fig. 1b). For each of the 192 screens, we typically obtained on the order of 1–30 positives. However, only around 20% of these positives were reproduced in a second screen of the array (Table 1a). Although the exact causes of this variability are not known, they appear to include an infrequent and protein-specific rearrangement of the DNA-binding domain plasmid to generate proteins that activate transcription on their own. As a consequence of this variability, we scored as putative interacting partners only those proteins that were identified in two independent screens, even though this criterion also resulted in the omission of some known interactions found only once. Overall, 87 of the 192 DNA-binding domain hybrids screened were identified in a putative

‖ Permanent address: Department of Genetics, Box 8232, Washington University Medical School, 4566 Scott Avenue, St Louis, Missouri 63110, USA.

protein–protein interaction, resulting in 281 interacting protein pairs (Table 1a).

High-throughput screens of an activation-domain library

As an alternative method of genomic two-hybrid analysis, we developed high-throughput screens based on a library made by pooling transformants containing the roughly 6,000 potential ORFs fused to the Gal4 activation domain. The hybrid proteins were derived similarly to those in the two-hybrid array, with each of the potential ORFs cloned separately into a Gal4 DNA-binding domain vector in addition to the Gal4 activation domain vector. The same PCR products and recipient plasmids were used to generate two collections of transformants, each consisting of 64 barcoded 96-well plates. Of the 6,144 ORFs, 5,345 (87%) were successfully cloned into both plasmids (Table 1b). Transformants from the Gal4 activation domain collection were then pooled to form an activation-domain library. To screen for protein interactions, we mated each DNA-binding domain hybrid transformant in duplicate to the activation domain library. Mating mixes were transferred to selective plates to select diploid cells that expressed interacting pairs and activated both reporter genes (*URA3* and *lacZ*). Experiments were conducted in 96-well assay plates using semi-automation and computerized sample tracking to perform such large-scale transformation and mating reactions quickly.

Overall, 817 yeast ORFs (15% of the successfully cloned yeast ORFs) were identified in a putative protein–protein interaction by this approach, resulting in 692 interacting protein pairs (Table 1b). To assess the coverage of the screens, we classified the interactions according to their frequency. Sixty-eight per cent of the putative interactions were identified in independent experiments (41%) or multiple times in a single experiment (27%). The remaining 32% of the interactions were identified only once during the screening process. This moderate coverage reflects the depth of the experiment determined by the number of colonies per mating submitted for sequence analysis. To complete this study in a timely and cost-effective manner, we selected only 12 colonies from each mating. This number was chosen to validate this genome-wide high-throughput approach as well as to generate significant data of scientific interest.

Comparison of the approaches

The array screens and the library screens gave different data sets (Table 2). Forty-five per cent of the 192 proteins used in the array screens yielded interactions, compared to 8% of the 5,345 potential ORFs in the library screens. Some of the difference in the number of proteins that resulted in positives with each approach is attributable to the nonrandom choice of proteins for the array screens (some categories of proteins, such as membrane proteins and metabolic enzymes, are less likely to yield interacting partners, whereas signalling proteins are more likely to). However, for proteins that identified at least one binding partner, the array screens gave an average of 3.3 positives per protein, whereas the library screens gave an average of 1.8. In addition, the 12 positive DNA-binding domain hybrids common to both screens yielded 48 putative interactions in the array screens and 14 in the library screens. Thus, although the library approach permits a much higher throughput, the array screens generate more candidate interactors. The higher yield of candidates in the array screens can be partially attributed to the stringency of the selection procedures; the His selection for 14 days in the array screens was less stringent than the Ura selection for 4 days in the library screens. More significantly, the pooling of activation-domain transformants may select against interactions that involve cells with reduced growth rate or mating ability, and sequence analysis of twelve positives may identify only strongly interacting pairs. In this regard, the array may facilitate the detection of interactions that result in very low reporter gene activation, in that a single positive array element on the two-hybrid selection plate may be composed of many small, slow-growing colonies. However, the

Table 1 Summary of experimental results

(a) Protein array

Description	Total
Yeast ORFs screened	192
Yeast ORF yielding reproducible interactions	87
Total discrete interacting protein pairs (reproduced in a second screen)	281

(b) High-throughput screens

Description	Total
Yeast ORF PCR products	6,144
Yeast ORFs cloned*	5,345
ORFs pooled to generate the activation domain library	5,341†
ORF activating transcription on their own	680
Yeast ORFs identified to have interactions‡	817
Total discrete interacting protein pairs	692
Interactions identified in independent experiments§	286
Interactions identified multiple times in a single experiment‖	186
Interactions identified only once	220

* Number of PCR products giving transformants in both plasmids (pOBD2 and pOAD).
† One yeast ORF activation domain construct was excluded from the pool owing to self-activation in a test screen (YJR009C — glyceraldehyde-3-phosphate dehydrogenase) and three yeast ORF activation domain constructs were excluded because they encoded proteins that could affect the selection process (YPL248C — Gal4, YML051W — Gal80 and YEL021W — Ura3).
‡ The total number of yeast ORFs found as interacting binding domain clones and/or interacting activation domain clones in the screens.
§ All screening experiments were performed in duplicate.
‖ Interactions that were identified several times in only one mating.

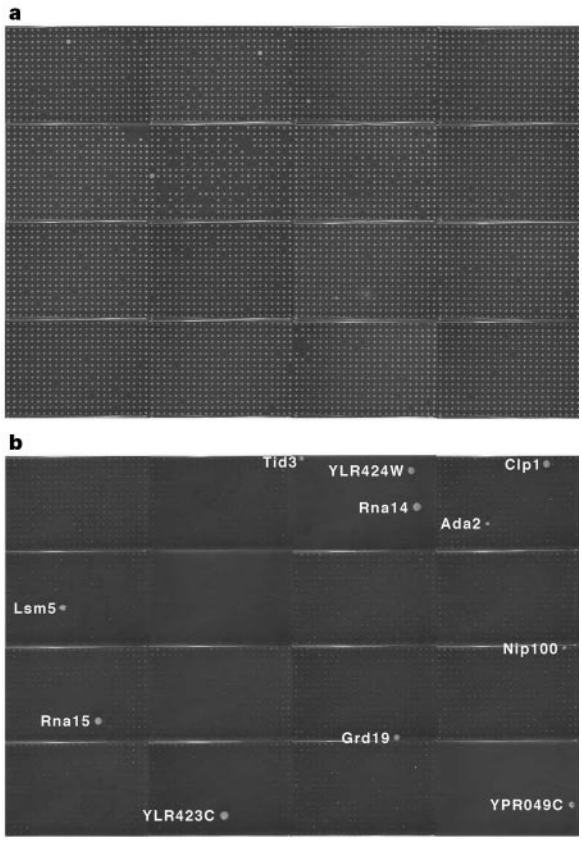

Figure 1 The two-hybrid assay carried out by screening a protein array. **a**, The array of ~6,000 haploid yeast transformants plated on medium lacking leucine, which allows growth of all transformants. Each transformant expresses one of the yeast ORFs expressed as a fusion to the Gal4 activation domain. **b**, Two-hybrid positives from a screen of the array with a Gal4 DNA-binding domain fusion of the Pcf11 protein, a component of the pre-mRNA cleavage and polyadenylation factor IA, which also consists of four other polypeptides[36]. Diploid colonies are shown after two weeks of growth on medium lacking tryptophan, leucine and histidine and supplemented with 3 mM 3-amino-1,2,4-triazole, thus allowing growth only of cells that express the *HIS3* two-hybrid reporter gene. Three other components of factor IA, Rna14, Rna15 and Clp1, were identified as Pcf11 interactors. Positives that do not appear in Table 2 were either not reproducible or are false positives that occurred in many screens.

array screens are much more labour- and material-intensive, and require several hours of robot time per screen, thus severely limiting the number of screens that can be performed.

We were interested in examining the putative protein–protein interactions identified in these screens in reference to their functional roles according to the yeast protein database (YPD) classification[10]. Representative proteins from 41 of the 43 YPD categories were identified in the screens (Table 3). Of the 1,004 active proteins, 412 fell into the 'unclassified' category. These 412 proteins yielded 509 distinct interactions, of which 164 (32%) were between proteins with no functional classification. This observation indicates that there may be a significant number of as yet undiscovered pathways and/or complexes that can be identified using systematic approaches. Results from both approaches were also compared with a compilation of literature-cited interactions (Table 2). From the 957 putative interactions identified by both approaches, at least 109 have been previously reported by others using two-hybrid, co-immunoprecipitation, copurification or affinity column techniques[2,10]. That only a subset of previously described interactions has been detected in our work can be attributed to specific features of the screens: the exclusive use of full-length proteins as both DNA-binding and activation-domain fusions and the versions of the two-hybrid system used, which include Gal4 as the DNA-binding domain fusion protein and centromeric plasmids. Each of these components can affect the sensitivity of the assay[11]. Additionally, sequence analysis of 200 ORF constructs used in constructing the array indicates that ~15% of the recombinant plasmids may lack insert, another ~3% may contain frameshifting errors, and about 5% of all colonies failed to grow. Thus, we estimate that the array contains ~85–90% of the yeast ORFs, given that each element is composed of two individual transformants.

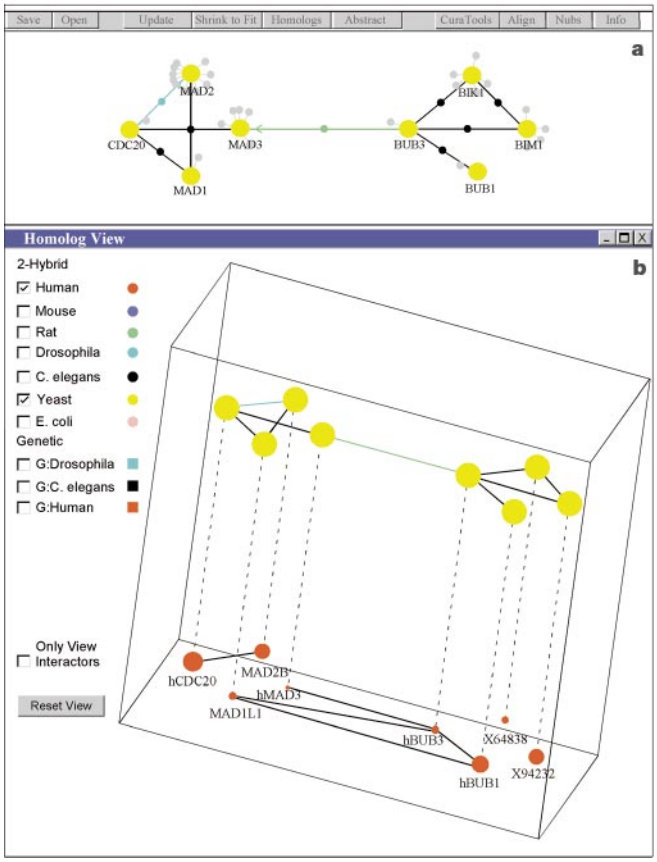

Figure 2 Data analysis software. **a**, The putative interaction identified between Mad3 and Bub3 which connects the spindle checkpoint complex[37] and the microtubule checkpoint complex[38]. Yeast proteins are shown as yellow spheres with the name of each gene indicated. Interactions in Figs 2 and 3 are shown as black lines (from literature), solid green lines (from library screens in independent matings), dashed green lines (from library screens in one mating), purple (from array screens) and blue lines (from literature and screens). Arrows point away from the protein used as the binding-domain clone when the interaction was identified. Grey nubs indicate other proteins that interact with that protein but have not been expanded. **b**, Same pathway shown using the homologue viewer; the pathway can be rotated and homologous proteins in human, mouse, rat, *Drosophila*, *Caenorhabditis elegans* and *Escherichia coli* can be displayed. Known interactions between proteins in other species can be viewed: for this pathway interactions between the human proteins hMad3/hBub3, hBub3/hBub1, hBub1/hMad1, hBub3/hMad1 and hCDC20/hMad2, shown in black, are reported in the literature[39–41]. The distance of each species protein icon (shown in key) from the yeast proteins (shown in yellow) represents the amount of overall similarity between the species. The size of the protein icon in each corresponding species indicates the amount of homology with the specific yeast protein. As the human homologues are highlighted in this example, their gene names are shown.

Results of the systematic two-hybrid screens

To examine the large number of potential interactions, we developed a new bioinformatics platform which, along with the complete set of data generated by these screens, is publicly available at http://portal.curagen.com. The software allows users to search for information on putative protein interactions identified in the screens or reported in the literature, to perform sequence analyses and view the results, to extend interactions to construct pathways and to view the homologues of the yeast genes in a number of species using the three-dimensional homologue viewer (see Fig. 2).

First, by using systematic approaches to analyse the yeast genome, we could identify interactions that place functionally unclassified proteins into a biological context. For example, two proteins of unknown function, YGR010W and YLR328W (77% identical), were observed to interact with each other. Additionally, both proteins bind to ornithine aminotransferase (Car2), indicating that they may be involved in arginine metabolism. Human ornithine aminotransferase (OATase) can complement an ornithine aminotransferase-deficient strain of *S. cerevisiae*, and mutations in human OATase cause gyrate atrophy of the choroid and retina[12].

Data from this study provide evidence of links between two proteins involved in autophagy, Apg13 and Apg1, and proteins of the Cvt (cytoplasm-to-vacuole targeting) pathway, Lap4, Vma22 and Vma6. Autophagy is a degradation pathway used under conditions of nutrient stress to nonselectively recycle cytoplasmic proteins and organelles to their constituent components, whereas the Cvt pathway is a biosynthetic pathway that transports the vacuolar enzyme aminopeptidase I (API, encoded by *LAP4*) specifically to the vacuole[13]. Several mutations in the Cvt pathway (*cvt*) and autophagocytosis (*aut* and *apg*) are allelic, indicating that both pathways may utilize some of the same molecular components[14]. Our study implicates a number of ORFs encoding proteins of unknown functions as potential components of autophagy (Fig. 3a). As several of the genes altered in *apg*, *aut* and *cvt* mutants have not yet been cloned, ORFs found in these interactions could be examined to determine whether they encode any of these genes. This study has also shown Lap4 to be a self-interactor, corroborating previous evidence that Lap4 assembles into a dodecamer[15], and the interaction between Apg1 and Apg13 lends support to previous genetic evidence indicating that *APG1* may be a high-copy suppressor of *apg13* (ref. 16).

Second, genome-wide two-hybrid approaches offer insight into novel interactions between proteins involved in the same biological function. For example, we screened four proteins (Lsm2, Lsm4, Lsm8 and Prp11) that are known or suspected to be involved in RNA splicing and that had been previously analysed or identified in another systematic set of two-hybrid screens[5] using a random library of activation-domain hybrids. Three of these contain the Sm1 and Sm2 motifs found in a core set of proteins associated with small nuclear RNAs (snRNAs) involved in splicing[17,18]; the yeast Sm proteins are homologous to the eight common Sm proteins identified

in mammalian cells. Screens of the three Sm proteins identified other Sm proteins (Table 2, Fig. 3b): the D1 homologue Lsm2 binds B (Lsm1), D2 (Smd2), E (Lsm5), F (Lsm6) and G (Lsm7) homologues; the D3 homologue Lsm4 binds B, F and G homologues and Lsm8; and Lsm8 binds D1, E, F and G homologues. These results support a proposed model[19] based on crystallographic, biochemical and genetic data, but also include interactions not predicted by the model and which might reflect exchangeability of proteins within the complex, additional contacts within or between subcomplexes, or bridging effects in the two-hybrid assay.

In yeast, diverse cyclins bind to Cdc28 in a coordinated manner to modulate its kinase activity during the cell cycle. The B-type cyclins are critical in the induction of bipolar mitotic spindle formation[20]. Each of the B-type cyclins, Clb1, Clb2 and Clb3, has been observed to be in a complex with Cks1 and Cdc28. Our observation of two-hybrid interactions between Cks1 and each of Clb1, Clb2 and Clb3 indicates that the kinase activity of Cdc28 could be regulated by cyclin Bs through their interaction with Cks1 (Fig. 3c).

Third, novel interactions that connect biological functions into larger cellular processes can be gleaned from our screens. The Sm proteins Lsm2, Lsm4 and Lsm8 identified ribosomal protein S28 (producing a signal with both Rps28a and Rps28b, the nearly identical copies of this protein), which may reflect an unusual involvement of Rps28 in splicing, or of the snRNP proteins in translation or ribosome biogenesis (Fig. 3b). Unexpectedly, a characterization of the mammalian spliceosome complex by two-dimensional gel separation and mass spectrometry identified a different ribosomal protein, Rps4x, as a previously unknown spliceosome-associated protein[21]. The three Sm proteins also interacted with Dcp1, a messenger RNA-decapping enzyme, consistent with the role of Lsm1 (Spb8) in decapping[22]. Finally, a screen with Dcp1 found Rps28b and thus provides further evidence for a functional interplay between these proteins. Both Lsm2 and Lsm8 identified Mtr3, implicated in mRNA transport[23], suggesting another possible link between splicing and other processes.

The meiosis-specific protein Msh5 is required for the resolution of crossovers during meiosis[24]. Meiotic recombination is initiated by double-strand breaks (DSBs), a prerequisite to crossover formation that is resolved in a structure called the synaptonemal complex. Mre11 is part of a complex that participates in DSB formation[25]. It is also known that Tid3 helps form the spindle pole body and interacts with Dmc1 (ref. 26), a protein that is required for the formation of the synaptonemal complex. We observed Msh5 to interact with both Mre11 and Tid3 (Fig. 3d). These novel associations tie DSB formation and the resolution of crossovers with Msh5 as the linking protein.

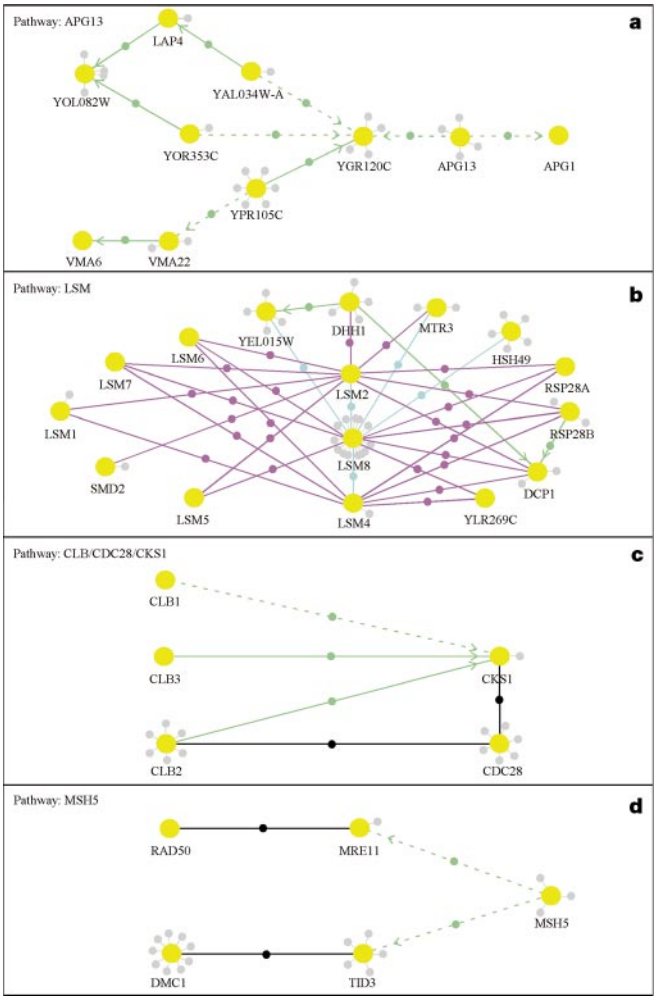

Figure 3 Expanded pathways shown using the software as described in the text. **a**, Autophagy pathway illustrating potential novel interactions that place functionally unclassified proteins in a biological context. **b**, Potential interactions identified by screens of the Sm motif-containing proteins Lsm2, Lsm4 and Lsm8. **c**, The Clb/Cdc28/Cks1 complex shows novel interactions between proteins involved in the same biological function. **d**, The Msh5 pathway illustrates novel interactions that link biological functions together into greater cellular processes.

Discussion

We have detected novel interactions for proteins previously screened by other workers who used the two-hybrid assay with activation-domain libraries of randomly generated inserts. Some of these new partners may reflect the comprehensive nature of the array and library approaches or the requirement for a full-length protein to detect some interactions. However, most of our data represent new potential interactions for proteins that have not been previously searched in the two-hybrid assay. Of the new interactions, many seem credible on the basis of genetic or other criteria, whereas the relevance of others cannot be easily assessed. However, some reproducible two-hybrid signals are unlikely to reflect true interactions, based on the known properties of the proteins involved. Thus, in the absence of other data, the set of proteins derived from each of these screens should be viewed as potential positives, serving to motivate other experiments that confirm or eliminate particular proteins as plausible interactors.

As part of these studies, we have developed a protein array approach as a new method for systematic genome-wide analysis. Arrays of biomolecules possess unique advantages for the handling and investigation of multiple samples. They provide a fixed location for each element such that those scoring positive in an assay are immediately identified; they have the capacity to be comprehensive and of high density; they can be screened by high-throughput robotic procedures using small volumes of reagents; and they allow the comparison of each assay value with the results of many other identical assays. Moreover, chemically pure protein arrays can be constructed by generating proteins fused to an affinity tag and recovering them by cell lysis and affinity purification[7]. The yeast activation-domain array and library described here also allow the detection *in vivo* of nucleic-acid–protein and small-molecule–protein interactions, through the use of hybrid molecules[27–31], in a manner similar to that for protein–protein interactions.

The publication of the complete genome sequence of *Caenorhabditis elegans* and the escalating efforts to complete the sequences of other genomes increase the need for high-throughput functional studies. The studies described here represent the first comprehensive biological screens that use the complete set of predicted ORFs from a eukaryotic organism. Both of the approaches could be scaled up for larger sets of proteins, such as those encoded by *Caenorhabditis elegans* or *Drosophila melanogaster*. The high-throughput library approach is reasonable to employ in order to complete a screen of all encoded ORFs for either of these organisms; however, the array approach, while much more time- and labour-intensive,

would probably provide more positives. The bioinformatics platform we have developed can incorporate new data sets as they become available and compare results across species to identify conserved interactions. Systematically applying multiple high-throughput strategies should increase our understanding of yeast and other eukaryotic organisms. □

Methods

Gap-repair cloning

We constructed transformants containing activation-domain hybrids by recombination[32] of the linearized vector pOAD[8] with PCR fragments corresponding to each of the yeast ORFs[8]. The DNA-binding domain vector pOBD2 was constructed by introducing 48 base pairs from pOAD[8], encoding residues 866–881 of the Gal4 activation domain, into pOBD[8] immediately 3′ to the DNA that encodes residue 147 of the Gal4 DNA-binding domain (S. McCraith and S.F., unpublished). This plasmid provides activation-domain sequences to allow cloning by recombination of the identical PCR fragments used to construct activation-domain hybrids. Transformation was carried out in a 96-well format using the lithium acetate procedure[33]. Yeast media were prepared as described[34].

Generation of the array. After transformation, cells were plated on 35-mm synthetic plates without leucine. The yeast recipient for the activation-domain hybrid plasmids was PJ69-4a (ref. 9), which is *MATa*. Two colonies from each transformation plate were pooled, cultured in liquid-leucine medium and transferred to solid-leucine medium in OmniTrays (Nalge Nunc International) by a Biomek 2000 Laboratory Automation Workstation (Beckman). We constructed an isogenic *MATα* derivative by switching the PJ69-4a strain using a plasmid carrying the *HO* gene. Selection for transformants carrying DNA-binding domain hybrids used synthetic plates without tryptophan.

Collections for the library screens. Five microlitres from individual transformations were grown on selective medium lacking leucine or tryptophan for two days at 30 °C. Patches of transformants were manually transferred into individual wells on micro-assay plates for further use. The yeast recipients were YULH (*MATa ura3-52 trp1 lys2 his3 leu2 gal4 gal80 GAL1–URA3 GAL1–lacZ*) for the Gal4 DNA-binding domain fusion in pOBD2 and N106r (*MATα ura3-52 his3 ade2 trp1 leu2 gal4 gal80 cyh2 lys2::GAL1–HIS3 ura3::GAL1–lacZ*) for the Gal4 AD fusion in pOAD.

Screening procedure

Array screening. Transformants of the a and α reporter strains were mated on YEPD plates for 2–3 days at 30 °C by transferring ~1 ml of an overnight culture of the *MATα* strain expressing a DNA-binding domain hybrid onto each of 16 OmniTrays using a 384-pin High Density Replicating Tool (Beckman), and then pinning the activation-domain array transformants of the *MATa* strain onto the same positions. Diploids were selected by transfer with the replicating tool to medium without leucine and tryptophan, followed by 2–3 days of further growth. For the two-hybrid selection, the diploids were transferred to medium without leucine, tryptophan and histidine supplemented with 3 mM 3-amino-1,2,4-triazole and scored after two weeks of growth at 30 °C. Further details about the array screening procedure are available at http://depts.washington.edu./sfields/.

Library screening. Mating reactions were performed on 96-well filter plates (Millipore MAHV S45) by mixing 10^7 *MATa* cells (Gal4 DNA-binding domain fusion) with 5×10^6 *MATα* cells (activation domain library) from liquid cultures in complete medium (YPAD). After filtration, the 96-well filter plates were incubated overnight at 30 °C on rectangular YPAD solid medium plates. We collected cells from the mating mixes from each filter with sterile water. A semi-automated Zymark work station was used throughout the cloning and screening procedures. Diploids containing potential interactors were selected for 4 days at 30 °C on medium lacking leucine, tryptophan and uracil, and simultaneously screened for lacZ expression by the addition of X-gal. Each mating generated 5×10^5 to 10^6 original diploids per well, suggesting that the library was covered 80–160 times. Up to 12 blue colonies were picked per mating, generating a collection of 96-well plates of diploid clones as the final product of the screening process. The activation-domain fusion plasmids were submitted for PCR amplification and sequencing to identify the yeast ORF. A total of 8,676 blue colonies were picked from the screens: 6,909 (80%) passed PCR, sequencing, vector trimming and 6,215 (72%) passed interaction quality control. The resulting sequences were compared with the yeast sequence database using Blast2 (ref. 35). Sample handling and manipulation during the screens was tracked by computer and data analysis was carried out using GeneScape, web-based software developed at CuraGen.

Received 6 September; accepted 29 November 1999.

1. Goffeau, A. *et al.* Life with 6000 genes. *Science* **274,** 546–567 (1996).
2. Mewes, H. W., Albermann, K., Heumann, K., Liebl, S. & Pfeiffer, F. MIPS: a database for protein sequences, homology data and yeast genome information. *Nucleic Acids Res.* **25,** 28–30 (1997).
3. Fields, S. & Song, O. A novel genetic system to detect protein–protein interactions. *Nature* **340,** 245–246 (1989).
4. Bartel, P. L., Roecklein, J. A., SenGupta, D. & Fields, S. A protein linkage map of *Escherichia coli* bacteriophage T7. *Nature Genet.* **12,** 72–77 (1996).
5. Fromont-Racine, M., Rain, J. C. & Legrain, P. Toward a functional analysis of the yeast genome through exhaustive two-hybrid screens. *Nature Genet.* **16,** 277–282 (1997).
6. Flores, A. *et al.* A protein–protein interaction map of yeast RNA polymerase III. *Proc. Natl Acad. Sci. USA* **96,** 7815–7820 (1999).
7. Martzen, M. R. *et al.* A biochemical genomics approach for identifying genes by the activity of their products. *Science* **286,** 1153–1155 (1999).
8. Hudson, J. R. Jr *et al.* The complete set of predicted genes from *Saccharomyces cerevisiae* in a readily usable form. *Genome Res.* **7,** 1169–1173 (1997).
9. James, P., Halladay, J. & Craig, E. A. Genomic libraries and a host strain designed for highly efficient two-hybrid selection in yeast. *Genetics* **144,** 1425–1436 (1996).
10. Hodges, P. E., McKee, A. H., Davis, B. P., Payne, W. E. & Garrels, J. I. The Yeast Proteome Database (YPD): a model for the organization and presentation of genome-wide functional data. *Nucleic Acids Res.* **27,** 69–73 (1999).
11. Legrain, P., Dokhelar, M. C. & Transy, C. Detection of protein–protein interactions using different vectors in the two-hybrid system. *Nucleic Acids Res.* **22,** 3241–3242 (1994).
12. Ramesh, V., Gusella, J. F. & Shih, V. E. Molecular pathology of gyrate atrophy of the choroid and retina due to ornithine aminotransferase deficiency. *Mol. Biol. Med.* **8,** 81–93 (1991).
13. Scott, S. V. & Klionsky, D. J. Delivery of proteins and organelles to the vacuole from the cytoplasm. *Curr. Opin. Cell Biol.* **10,** 523–529 (1998).
14. Scott, S. V. *et al.* Cytoplasm-to-vacuole targeting and autophagy employ the same machinery to deliver proteins to the yeast vacuole. *Proc. Natl Acad. Sci. USA* **93,** 12304–12308 (1996).
15. Funakoshi, T., Matsuura, A., Noda, T. & Ohsumi, Y. Analyses of APG13 gene involved in autophagy in yeast, *Saccharomyces cerevisiae*. *Gene* **192,** 207–213 (1997).
16. Kim, J., Scott, S. V., Oda, M. N. & Klionsky, D. J. Transport of a large oligomeric protein by the cytoplasm to vacuole protein targeting pathway. *J. Cell Biol.* **137,** 609–618 (1997).
17. Kramer, A. The structure and function of proteins involved in mammalian pre-mRNA splicing. *Annu. Rev. Biochem.* **65,** 367–409 (1996).
18. Mayes, A. E., Verdone, L., Legrain, P. & Beggs, J. D. Characterization of Sm-like proteins in yeast and their association with U6 snRNA. *EMBO J.* **18,** 4321–4331 (1999).
19. Kambach, C. *et al.* Crystal structures of two Sm protein complexes and their implications for the assembly of the spliceosomal snRNPs. *Cell* **96,** 375–387 (1999).
20. Nasmyth, K. Control of the yeast cell cycle by the Cdc28 protein kinase. *Curr. Opin. Cell Biol.* **5,** 166–179 (1993).
21. Neubauer, G. *et al.* Mass spectrometry and EST-database searching allows characterization of the multi-protein spliceosome complex. *Nature Genet.* **20,** 46–50 (1998).
22. Boeck, R., Lapeyre, B., Brown, C. E. & Sachs, A. B. Capped mRNA degradation intermediates accumulate in the yeast spb8-2 mutant. *Mol. Cell. Biol.* **18,** 5062–5072 (1998).
23. Kadowaki, T. *et al.* Isolation and characterization of *Saccharomyces cerevisiae* mRNA transport-defective (mtr) mutants. *J. Cell Biol.* **126,** 649–659 (1994). [Published erratum appears in *J. Cell Biol.* **126,** 1627.]
24. Hollingsworth, N. M., Ponte, L. & Halsey, C. MSH5, a novel MutS homolog, facilitates meiotic reciprocal recombination between homologs in *Saccharomyces cerevisiae* but not mismatch repair. *Genes Dev.* **9,** 1728–1739 (1995).
25. Usui, T. *et al.* Complex formation and functional versatility of Mre11 of budding yeast in recombination. *Cell* **95,** 705–716 (1998).
26. Bishop, D. K., Park, D., Xu, L. & Kleckner, N. DMC1: a meiosis-specific yeast homolog of *E. coli* recA required for recombination, synaptonemal complex formation, and cell cycle progression. *Cell* **69,** 439–456 (1992).
27. SenGupta, D. J. *et al.* A three-hybrid system to detect RNA–protein interactions *in vivo*. *Proc. Natl Acad. Sci. USA* **93,** 8496–8501 (1996).
28. Wang, M. M. & Reed, R. R. Molecular cloning of the olfactory neuronal transcription factor Olf-1 by genetic selection in yeast. *Nature* **364,** 121–126 (1993).
29. Li, J. J. & Herskowitz, I. Isolation of ORC6, a component of the yeast origin recognition complex by a one-hybrid system [see comments]. *Science* **262,** 1870–1874 (1993).
30. Licitra, E. J. & Liu, J. O. A three-hybrid system for detecting small ligand–protein receptor interactions. *Proc. Natl Acad. Sci. USA* **93,** 12817–12821 (1996).
31. Belshaw, P. J., Ho, S. N., Crabtree, G. R. & Schreiber, S. L. Controlling protein association and subcellular localization with a synthetic ligand that induces heterodimerization of proteins. *Proc. Natl Acad. Sci. USA* **93,** 4604–4607 (1996).
32. Ma, H., Kunes, S., Schatz, P. J. & Botstein, D. Plasmid construction by homologous recombination in yeast. *Gene* **58,** 201–216 (1987).
33. Ito, H., Fukuda, Y., Murata, K. & Kimura, A. Transformation of intact yeast cells treated with alkali cations. *J. Bacteriol.* **153,** 163–168 (1983).
34. Sherman, F., Fink, G. R. & Hicks, J. B. *Methods in Yeast Genetics* (Cold Spring Harbor Laboratory, Cold Spring Harbor, 1986).
35. Altschul, S. F., Gish, W., Miller, W., Myers, E. W. & Lipman, D. J. Basic local alignment search tool. *J. Mol. Biol.* **215,** 403–410 (1990).
36. Minvielle-Sebastia, L., Preker, P. J., Wiederkehr, T., Strahm, Y. & Keller, W. The major yeast poly(A)-binding protein is associated with cleavage factor IA and functions in premessenger RNA 3′-end formation. *Proc. Natl Acad. Sci. USA* **94,** 7897–7902 (1997).
37. Hwang, L. H. *et al.* Budding yeast Cdc20: a target of the spindle checkpoint. *Science* **279,** 1041–1044 (1998).
38. Guenette, S., Magendantz, M. & Solomon, F. Suppression of a conditional mutation in alpha-tubulin by overexpression of two checkpoint genes. *J. Cell Sci.* **108,** 1195–1204 (1995).
39. Hoyt, M. A., Totis, L. & Roberts, B. T. *S. cerevisiae* genes required for cell cycle arrest in response to loss of microtubule function. *Cell* **66,** 507–517 (1991).
40. Seeley, T. W., Wang, L. & Zhen, J. Y. Phosphorylation of human MAD1 by the BUB1 kinase in vitro. *Biochem. Biophys. Res. Commun.* **257,** 589–595 (1999).
41. Kallio, M., Weinstein, J., Daum, J. R., Burke, D. J. & Gorbsky, G. J. Mammalian p55CDC mediates association of the spindle checkpoint protein Mad2 with the cyclosome/anaphase-promoting complex, and is involved in regulating anaphase onset and late mitotic events. *J. Cell Biol.* **141,** 1393–1406 (1998).

Acknowledgements

We thank K. Furtak, J. Gilbert, N. Huber, M. Laurino, L. Matthies, A. Perna, C. Pratt and B. Rittman for technical assistance; B. Drees, R. Hughes and S. McCraith for help with some of the experiments; P. Hodges (Proteome) for providing a compilation of protein interactions; and B. Byers, M. Olson, R. Franza, M. Roth, D. Lewin, T. Jarvie and J. Simons for comments on the manuscript. S.F. is supported by grants from the NIH and the Merck Genome Research Institute. P.U. is supported by a fellowship from the Deutscher Akademischer Austauschdienst (DAAD). S.F. is an investigator of the Howard Hughes Medical Institute.

Correspondence and requests for materials should be addressed to J.R. (e-mail: jrothberg@curagen.com) and S.F. (e-mail: fields@u.washington.edu).

Table 2 List of the 957 interactions identified in both two-hybrid screens

BD fusion	AD fusion	Source
ADE2 (nm)	ADE2 (nm)	*
ADE2 (nm)	RAD18 (ri)	*
ADE2 (nm)	SED4 (vt)	*
ADE2 (nm)	YBR134W (un)	*
ADE6 (nm)	YLR386W (un)	*
ADE8 (nm)	MED4 (p2)	*
ADE8 (nm)	SOH1 (un)	*
ADE8 (nm)	YCR063W (un)	*
ADH2 (cm)	YFL042C (un)	†
AHC1 (ch,p2)	YCR082W (un)	*
AIP1 (st)	APC9 (cc,mi,pd)	*
ALR1 (sm)	GCD7 (ps)	*
ALR1 (sm)	PGD1 (p2)	*
ALR1 (sm)	YGL024W (un)	*
ALR1 (sm)	YNL086W (un)	*
APG12 (pd,pm,vt)	AUT1 (cs,pt)	†
APG12 (pd,pm,vt)	SAP18 (pd)	*
APG13 (pd,vt)	APG1 (me,pd,vt)	*
APG13 (pd,vt)	PUP2 (pd)	*
APG13 (pd,vt)	SEC35 (vt)	*
APG13 (pd,vt)	YNL086W (un)	*
APG5 (pd,vt)	APG12 (pd,pm,vt)	*,†¶,∫
APG5 (pd,vt)	SAP18 (pd)	*
APG7 (di,pd,pt)	APG12 (pd,pm,vt)	*,‡
APG7 (di,pd,pt)	AUT1 (cs,pt)	*
APG7 (di,pd,pt)	AUT7 (me,pd,vt)	*
APM1 (vt)	APL2 (vt)	*,∫
APM2 (vt)	APL2 (vt)	*
ARH1 (en)	CDC39 (cc,p2)	*
ARH1 (en)	GIF1 (cc)	*
ARP10 (st)	ARP1 (mi)	*
ATP20 (en,sm)	SHE2 (cp,di)	*
BEM4 (cp,si)	SCS3 (li)	*
BEM4 (cp,si)	YIL163C (un)	*
BEM4 (cp,si)	YLR049C (un)	*
BMH2 (di,si)	BOP3 (un)	*
BMH2 (di,si)	ECM13 (wm)	*
BUB2 (cc)	DDI1 (vt)	†
BUB2 (cc)	GIC1 (cp,mr)	†
BUB2 (cc)	YGR153W (un)	†
BUB2 (cc)	YNL335W (un)	†
BUB3 (cc)	MAD3 (cc)	*
BUD6 (cp)	YGL015C (un)	*
CAF20 (ps)	CDC33 (cc,ps)	*,∫
CAR1 (aa,om)	CAR1 (aa,om)	†
CAR2 (aa,om)	SNF6 (ch,p2)	*
CAR2 (aa,om)	YGR010W (un)	*
CAR2 (aa,om)	YLR328W (nm)	*
CDC13 (ch)	STN1 (ch)	†,‡
CDC20 (mr,mi)	MAD2 (cc,mi)	*,‡
CDC33 (cc,ps)	CAF20 (ps)	*,∫
CDC42 (cp,st,mr)	BEM4 (cp,si)	†,‡
CDC42 (cp,st,mr)	RDI1 (un)	*
CDC43 (pm)	RAM2 (mr,pm)	*,∫
CDC53 (aa,cc,pd)	CDC7 (ch,ri,ds,me,rc)	†
CDC53 (aa,cc,pd)	SKP1 (aa,cc,ch,pd)	†,∫
CDC53 (aa,cc,pd)	YLR100W (un)	†
CDC53 (aa,cc,pd)	YLR128W (un)	†
CDC53 (aa,cc,pd)	YLR368W (un)	†,†¶
CDC53 (aa,cc,pd)	ZIP2 (me,rc)	†
CDC7 (ch,ri,ds,me,rc)	ARG3 (aa,om)	*
CDC7 (ch,ri,ds,me,rc)	DHH1 (rp)	*
CDC7 (ch,ri,ds,me,rc)	PTM1 (un)	*
CDC7 (ch,ri,ds,me,rc)	TEL2 (ch)	*
CDC7 (ch,ri,ds,me,rc)	YCR022C (un)	*
CDC7 (ch,ri,ds,me,rc)	YCR050C (un)	*
CDC7 (ch,ri,ds,me,rc)	YEL023C (un)	*
CDC7 (ch,ri,ds,me,rc)	YFR057W (un)	*
CDC7 (ch,ri,ds,me,rc)	YNR048W (un)	*
CDC7 (ch,ri,ds,me,rc)	YOR006C (un)	*
CDD1 (nm)	CDD1 (nm)	*
CHK1 (cc)	GFD1 (un)	*
CHK1 (cc)	GSY2 (cm)	*
CIN4 (mr,mi)	GYP1 (vt)	†
CIN4 (mr,mi)	YBR284W (un)	†
CIT2 (en)	CIT2 (en)	†,*
CIT2 (en)	MHP1 (un)	†
CKA2 (p2)	CKB2 (p3)	*
CLB1 (cc)	CKS1 (cc)	*
CLB2 (cc)	CKS1 (cc)	*
CLB2 (cc)	FPR1 (un)	*
CLB2 (cc)	MUS81 (ri)	*
CLB2 (cc)	YDR412W (un)	*
CLB2 (cc)	YHR035W (un)	*
CLB2 (cc)	YNR022C (un)	*
CLB3 (cc)	CKS1 (cc)	*
CLN3 (cc)	MAD3 (cc)	*
CNA1 (cp,mr,si,sm)	YNL047C (un)	*
CNB1 (om,sm)	YMR211W (un)	†
CNS1 (un)	STP1 (rp,sm)	†
COF1 (st,vt)	ACT1 (cp,st,vt)	†,∫
CPA1 (aa)	CKB2 (p3)	*
CPR6 (pf)	HYR1 (cs)	*
CRN1 (un)	SKP1 (aa,cc,ch,pd)	*
CSE2 (cc,mi,p2)	MED4 (p2)	*,∫
CTF13 (cc,ch,mi)	AQY2 (sm)	†
CTF13 (cc,ch,mi)	YOR359W (un)	†
CYP2 (cs,vt)	JSN1 (st)	*
CYS4 (aa)	YCR086W (me)	*
DAL3 (om)	DAL3 (om)	*
DAL82 (om,p2)	DAL82 (om,p2)	*
DAM1 (mi)	DUO1 (un)	*,‡
DCP2 (p2)	DCP1 (rt)	*
DCP2 (p2)	YEL015W (un)	*
DHH1 (rp)	DCP1 (rt)	*
DHH1 (rp)	YEL015W (un)	*
DIB1 (mi,rp,rs)	PRP6 (rp,rs)	*,∫
DIG1 (di)	DIG2 (di)	*
DMC1 (me,rc)	DMC1 (me,rc)	*,‡
DNA43 (ds)	MCM6 (ds)	*,‡
DUO1 (un)	BIM1 (cc,mi)	*
DUO1 (un)	YDR016C (un)	*
EBS1 (un)	DCP1 (rt)	*
EBS1 (un)	GAL83 (cm)	*
EBS1 (un)	MAD2 (cc,mi)	*
EBS1 (un)	MUM2 (me)	*
EBS1 (un)	STD1 (cm,cs,sm)	*
ECI2 (li)	ECI1 (li)	*
ECM19 (wm)	TAF61 (p2)	*
ECM31 (wm)	ECM31 (wm)	*
ENT3 (un)	YOR111W (un)	*
EST1 (ch,ds)	MCM6 (ds)	†
EST1 (ch,ds)	SPT23 (ch)	†
EST1 (ch,ds)	URE2 (aa,om,p2)	†
EST1 (ch,ds)	YAL028W (un)	†
EST1 (ch,ds)	YGR160W (un)	†
EST1 (ch,ds)	YJL019W (un)	†
EST1 (ch,ds)	YMD8 (sm)	†
FAP1 (un)	MRE11 (wm,ch,ri,me,rc)	*
FAP1 (un)	SHE2 (cp,di)	*
FAR3 (cc,mr)	YFR008W (un)	*
FMN1 (om)	YDR398W (un)	*
FOL2 (om)	FOL2 (om)	*
FPR1 (un)	HOM3 (aa)	*,‡
FPR1 (un)	YMR087W (un)	†
FUI1 (nm,sm)	RPN3 (pd)	*
FUN20 (rs,rp)	YLR345W (cm)	*
FUN20 (rs,rp)	YPL151C (un)	*
FUR1 (nm)	APG13 (pd,vt)	*
FZF1 (om,p2)	CKB2 (p3)	*
FZF1 (om,p2)	PHO12 (ph)	*
FZF1 (om,p2)	TFC4 (p3)	*
GCD7 (ps)	YPL070W (un)	*
GCN3 (ps)	GCN3 (ps)	*
GCN5 (ch,p2,pm)	ADA2 (p2)	*,‡
GDH1 (aa)	LSM1 (rp,rs)	*
GFD1 (un)	NAB2 (nc,rp)	*
GIM5 (st,pf)	YKE2 (st)	*,∫
GIS4 (un)	CUP2 (cs,p2)	*
GLC7 (cm,cs,me,mi)	BDF2 (ch)	†
GLC7 (cm,cs,me,mi)	BNI4 (wm,ck)	†,*
GLC7 (cm,cs,me,mi)	GIP1 (me)	†,‡
GLC7 (cm,cs,me,mi)	MHP1 (un)	†
GLC7 (cm,cs,me,mi)	PAN1 (cp,st,vt)	†
GLC7 (cm,cs,me,mi)	REF2 (rp)	†
GLC7 (cm,cs,me,mi)	SCD5 (vt)	†,‡
GLC7 (cm,cs,me,mi)	YDR130C (un)	†
GLC7 (cm,cs,me,mi)	YDR412W (un)	†
GLC7 (cm,cs,me,mi)	YHR100C (un)	†
GLC7 (cm,cs,me,mi)	YOR315W (un)	†
GLG2 (cm)	GLG2 (cm)	*
GLK1 (cm)	ARGR2 (aa)	*
GLK1 (cm)	FIG1 (mr)	*
GPD2 (cm)	GNA1 (cc,wm)	*
GRX3 (cs)	RCS1 (sm)	*
GRX5 (cs)	YIL105C (un)	*
GRX5 (cs)	YNL047C (un)	*
GSG1 (me)	YHB1 (un)	*
GSP1 (nc)	MOG1 (nc)	*,‡
GSP2 (nc)	MOG1 (nc)	*
GTR1 (sm)	GTR1 (sm)	*
GZF3 (om,p2)	HDA1 (ch,pm)	*
HAP2 (cm,en,p2)	HAP3 (p2)	*,‡
HAP2 (cm,en,p2)	HAP5 (p2)	*,‡
HAP3 (p2)	HAP5 (p2)	*,‡
HEX3 (cm)	SMT3 (pm)	*,†¶
HEX3 (cm)	YER116C (un)	*
HIS3 (aa)	HIS3 (aa)	*
HOR2 (cm,cs)	YPL201C (un)	*
HPR5 (ri)	GDS1 (un)	*
HPR5 (ri)	MEL1 (cm)	*
HPR5 (ri)	SMT3 (pm)	*
HPR5 (ri)	YDR078C (un)	*
HRP1 (rp)	NAB2 (nc,rp)	*
HRR25 (ri)	ADY1 (un)	*
HRT1 (pm)	YAK1 (cc,cs)	*
HRT1 (pm)	YIL001W (un)	*
HRT1 (pm)	YJL200C (un)	*
HSH49 (rp,rs)	YBR103W (ch)	†
HST3 (ch)	SFP1 (cc,nc)	*
HTA1 (ch,p2)	NAP1 (ch)	†,*
HTA3 (ch)	YJL019W (un)	†
IME4 (me,p2)	MUM2 (me)	*
INO4 (li,p2)	APL2 (vt)	*
INO4 (li,p2)	HCS1 (ds)	*
INO4 (li,p2)	INO2 (li,mi)	*,‡
INO4 (li,p2)	YMR317W (un)	*
INO4 (li,p2)	YNL279W (un)	*
INO80 (un)	GDS1 (un)	*
INO80 (un)	NHP10 (un)	*
IPK1 (li,nc)	RPS28B (ps)	*
IPK1 (li,nc)	STE24 (pm)	*
IPK1 (li,nc)	YLR323C (un)	*
IPK1 (li,nc)	YOR078W (un)	*
IRE1 (cs,om,si)	YDR532C (un)	†
ISA1 (un)	RPS26A (ps)	*
ISA1 (un)	RPS26B (ps)	*
ISC10 (me)	TRP5 (aa)	*
ISU2 (un)	YPL088W (un)	*
KAP104 (nc)	YNR069C (un)	†
KAR4 (mr)	MUM2 (me)	*
KCS1 (p2)	BMH2 (di,si)	*
KEL1 (cp,mr)	CAF17 (p2)	*
KEL1 (cp,mr)	STD1 (cm,cs,sm)	*
KEL1 (cp,mr)	YMR181C (un)	*
KGD2 (cm)	SMT3 (pm)	*
KIN1 (un)	YOL082W (un)	*
KRR1 (un)	MCM6 (ds)	*
KSS1 (mr,si)	STE7 (di,mr)	†,‡
LAP4 (pd)	LAP4 (pd)	*,∫
LAP4 (pd)	YOL082W (un)	*
LCP5 (rp)	BFR2 (pt)	*
LEU4 (aa)	YKL183W (un)	*
LOS1 (nc)	RPC25 (p3)	†
LPP1 (li)	SHE2 (cp,di)	*
LRS4 (p1)	YCR086W (me)	*
LSM2 (rp,rs)	DCP1 (rt)	†
LSM2 (rp,rs)	DHH1 (rp)	†
LSM2 (rp,rs)	LSM1 (rp,rs)	†,‡
LSM2 (rp,rs)	LSM5 (rp,rs)	†,‡
LSM2 (rp,rs)	LSM6 (rp,rs)	†,‡
LSM2 (rp,rs)	LSM7 (rp,rs)	†,‡
LSM2 (rp,rs)	MTR3 (rp)	†
LSM2 (rp,rs)	RPS28A (ps)	†
LSM2 (rp,rs)	RPS28B (ps)	†
LSM2 (rp,rs)	SMD2 (ch,ds,rp,rs)	†,‡
LSM4 (rp,rs)	CKB2 (p3)	†
LSM4 (rp,rs)	DCP1 (rt)	†
LSM4 (rp,rs)	LSM1 (rp,rs)	†,‡
LSM4 (rp,rs)	LSM6 (rp,rs)	†,∫
LSM4 (rp,rs)	LSM7 (rp,rs)	†,∫
LSM4 (rp,rs)	LSM8 (rp,rs)	†,∫
LSM4 (rp,rs)	RPS28A (ps)	†
LSM4 (rp,rs)	RPS28B (ps)	†
LSM4 (rp,rs)	YLR269C (un)	†
LSM8 (rp,rs)	DCP1 (rt)	†
LSM8 (rp,rs)	DSS4 (vt)	†
LSM8 (rp,rs)	HSH49 (rp,rs)	†,‡
LSM8 (rp,rs)	LSM2 (rp,rs)	†,‡
LSM8 (rp,rs)	LSM5 (rp,rs)	†,‡
LSM8 (rp,rs)	LSM6 (rp,rs)	†,‡
LSM8 (rp,rs)	LSM7 (rp,rs)	†,‡
LSM8 (rp,rs)	MTR3 (rp)	†
LSM8 (rp,rs)	RPS28A (ps)	†
LSM8 (rp,rs)	RPS28B (ps)	†
LSM8 (rp,rs)	YEL015W (un)	†,‡
LSM8 (rp,rs)	YLR269C (un)	†
LST7 (vt)	PUT3 (aa)	*
LYS5 (aa)	FZF1 (om,p2)	*
MAK3 (pm)	MAK10 (en,ot)	*
MAK31 (rt)	MAK10 (en,ot)	*
MCM16 (mi)	MCM22 (ch)	*
MCM22 (ch)	MCM16 (mi)	*
MEC3 (cc)	SAP18 (pd)	*
MED11 (p2)	SRB6 (p2)	*
MED7 (p2)	MED4 (p2)	*,∫
MER1 (rp,rc)	MRP8 (ps)	*
MET18 (aa,ri,p2)	MED11 (p2)	†
MET30 (aa,om,pd)	HDR1 (me)	†
MET30 (aa,om,pd)	MNS1 (pm)	†
MET30 (aa,om,pd)	SRL2 (un)	†
MET30 (aa,om,pd)	YBR270C (un)	†
MET30 (aa,om,pd)	YEL015W (un)	†
MET30 (aa,om,pd)	YJL058C (un)	†
MET31 (aa,p2)	GCN4 (aa,nm,p2)	*
MIG1 (cm,p2,si)	YPL025C (un)	†
MKK2 (cs)	SLT2 (cs,wm,si)	*,‡
MOB2 (cc)	YOL036W (un)	*
MOG1 (nc)	GSP2 (nc)	*
MPD2 (pf)	MSR1 (ps)	*
MPD2 (pf)	YLR312C (un)	*
MRP8 (ps)	MRP8 (ps)	*
MRP8 (ps)	SMP2 (wm,en)	*
MSB2 (cp)	CDC36 (cc,p2)	*
MSB2 (cp)	MAD2 (cc,mi)	*
MSB2 (cp)	MAD3 (cc)	*
MSB2 (cp)	NIP7 (rp)	*
MSB2 (cp)	TID3 (mi)	*
MSH5 (me,rc)	HSL7 (cc)	*
MSH5 (me,rc)	MRE11 (wm,ch,ri,me,rc)	*
MSH5 (me,rc)	PGD1 (p2)	*

BD fusion	AD fusion	Source
MSH5 (me,rc)	TID3 (mi)	*
MSH5 (me,rc)	YGL170C (cm)	*
MSN5 (mr,nc)	HMO1 (ch)	†
MSN5 (mr,nc)	SEC9 (vt)	†
MSN5 (mr,nc)	SWI5 (cc,ch)	*
MSN5 (mr,nc)	YOR359W (un)	†
MSN5 (mr,nc)	YPR008W (un)	†
MTR3 (rp)	RRP42 (rp,rt)	*
MTW1 (un)	LAP4 (pd)	*
MTW1 (un)	NUP49 (nc)	*
MTW1 (un)	SEC35 (vt)	*
NAB2 (nc,rp)	GCN3 (ps)	*
NDC1 (mi)	ASM4 (ds,nc)	*
NDC1 (mi)	NUP53 (nc)	*
NHP10 (un)	YER092W (un)	*
NIC96 (nc)	NUP53 (nc)	*
NIC96 (nc)	SEC35 (vt)	*
NIF3 (p2,pm)	NIF3 (p2,pm)	*
NIP1 (ps)	SUI1 (ps)	*,‡
NIP1 (ps)	YNL047C (un)	*
NIP1 (ps)	YOR284W (un)	*
NIP100 (mi,nc)	ARP1 (mi)	*,ʃ
NIP100 (mi,nc)	TID3 (mi)	*
NIP100 (mi,nc)	YJL184W (un)	*
NPL4 (nc)	UFD1 (pd)	*
NPL6 (nc)	RSC8 (ch,p2)	*
NTH1 (cm,cs)	YLR270W (un)	*
NUF2 (mi)	PRS2 (aa,nm)	*
NUP157 (nc)	MAD2 (cc,mi)	*
NUP157 (nc)	NUP53 (nc)	*
NUP157 (nc)	YEL015W (un)	*
NUP2 (nc)	HSP10 (pf)	†
NUP57 (nc)	NSP1 (nc)	*
NUP57 (nc)	NUP49 (nc)	*
NUP57 (nc)	TAF17 (p2)	*
PAC1 (st)	YLR254C (un)	*
PCF11 (rp)	ADA2 (p2)	†
PCF11 (rp)	CLP1 (rp)	†,‡
PCF11 (rp)	RNA14 (rp)	†,‡
PCF11 (rp)	RNA15 (rp)	†,‡
PCF11 (rp)	YLR423C (un)	†
PCF11 (rp)	YLR424W (un)	†
PCF11 (rp)	YPR049C (un)	†
PCL10 (cm)	PHO85 (ph,si)	*,†¶,‡
PCL2 (cc)	SWI5 (cc,ch)	*
PCL6 (un)	YJL084C (un)	*
PCL6 (un)	YLR190W (un)	*
PDB1 (cm,en)	YLR345W (cm)	*
PDR11 (sm)	HMO1 (ch)	*
PEX7 (li,pt)	PEX18 (pt)	*,‡
PEX7 (li,pt)	PEX21 (pt)	*,‡
PEX7 (li,pt)	POT1 (li)	*,‡
PFK1 (cm)	UBP8 (pd)	†
PHO85 (ph,si)	CLG1 (un)	†,‡
PHO85 (ph,si)	PCL2 (cc)	†,‡
PHO85 (ph,si)	PCL6 (un)	†,‡
PHO85 (ph,si)	PCL7 (un)	†,‡
PHO85 (ph,si)	PCL8 (cm)	†,‡
PHO85 (ph,si)	PCL9 (cc)	†,‡
PHO85 (ph,si)	SOR1 (cm)	†
PHO85 (ph,si)	YDL246C (cm)	†
PHO85 (ph,si)	YNL201C (cm)	†
PIB1 (vt)	YPL133C (un)	*
PKC1 (wm,si)	ZDS2 (cc)	*
PKH1 (si)	YHR207C (un)	*
PKH1 (si)	YIR044C (un)	*
PKH1 (si)	YRF1-4 (ch)	*
POM152 (nc)	IKS1 (un)	*
POM152 (nc)	NUP53 (nc)	*
PPA2 (ph)	GCN3 (ps)	*
PPG1 (cm)	CPR6 (pf)	†
PPG1 (cm)	HSC82 (cs,ot)	†
PPG1 (cm)	PPT1 (un)	†
PPT1 (un)	ADR1 (p2)	†
PRB1 (pd)	YML032CA (un)	*
PRE10 (pd)	GNA1 (cc,wm)	*
PRE3 (pd)	YLR386W (un)	*
PRE5 (pd)	SHE2 (cp,di)	*
PRO3 (aa)	PRO3 (aa)	*
PRP11 (rp,rs)	PRP21 (rp,rs)	†,‡
PRP5 (rp,rs)	SNF11 (ch,p2)	*
PRP6 (rp,rs)	DIB1 (mi,rp,rs)	†,*,ʃ
PRP6 (rp,rs)	UBC9 (cc,pd,pm)	†
PRS5 (aa,nm)	PRS2 (aa,nm)	*,‡
PSE1 (nc)	APL2 (vt)	†
PSE1 (nc)	HSP10 (pf)	†
PSE1 (nc)	KGD2 (cm)	†
PSE1 (nc)	NUP57 (nc)	†,ʃ
PSE1 (nc)	SOR1 (cm)	†
PSE1 (nc)	WTM2 (me,p2)	†
PSE1 (nc)	YDL246C (cm)	†
PSE1 (nc)	YER045C (un)	†
PSE1 (nc)	YIR025W (un)	†
PSE1 (nc)	YMR048W (un)	†
PSE1 (nc)	YPL133C (un)	†
PTC1 (rp,si)	NBP2 (ch)	*
PTC2 (si)	YDR071C (un)	†
PUT4 (aa,sm)	MTF1 (mt)	*
PUT4 (aa,sm)	YCR045C (pd)	*
PUT4 (aa,sm)	YJL084C (un)	*
PUT4 (aa,sm)	YLR294C (un)	*
RAD10 (ri,rc)	GCD1 (ps)	†
RAD10 (ri,rc)	YCR086W (me)	†
RAD17 (cc,ri)	MEC3 (cc)	*,ʃ
RAD4 (ri)	RAD23 (ri)	†,‡
RAD4 (ri)	RPS31 (ca,ps)	†
RAD51 (ri,rc)	SAP1 (ch)	†
RAD51 (ri,rc)	UBC9 (cc,pd,pm)	†
RAD51 (ri,rc)	YMR233W (un)	†
RAD51 (ri,rc)	YPL238C (un)	†
RAD51 (ri,rc)	YPR011C (sm)	†
RAD55 (ri,mi,rc)	RAD51 (ri,rc)	*,‡
RAD6 (ch,ri,me,pd,pm,rc)	RAD18 (ri)	*,ʃ
RAM1 (mr,pm)	RAM2 (mr,pm)	*,ʃ
RCK1 (un)	HOG1 (cs,si)	*
RGA1 (cp,mr)	YHL042W (un)	*
RGA1 (cp,mr)	YJL185C (un)	*
RGR1 (p2)	PEX19 (li)	*
RHO1 (cc,si)	BEM4 (cp,si)	†,‡
RHO4 (cp)	BEM4 (cp,si)	†,‡
RIM101 (di,me,p2)	ZAP1 (p2)	*
RIM11 (me)	IME1 (me,p2)	*,‡
RLF2 (ch)	MSI1 (ch,ri)	*,ʃ
RNP1 (rp)	YFR047C (aa,om)	*
RPB10 (p1,p2,p3,ca)	CUP2 (cs,p2)	*
RPC19 (p1,p3)	GTR1 (sm)	†
RPC19 (p1,p3)	YFR011C (un)	†
RPC19 (p1,p3)	YHL018W (un)	†
RPC19 (p1,p3)	YLR266C (p2)	†
RPC40 (p1,p3)	RPC19 (p1,p3)	*,†¶, ‡
RPC40 (p1,p3)	YLR238W (un)	*
RPC53 (p3)	YKR025W (un)	*
RPN11 (pd)	RPN8 (pd)	†,ʃ
RPN12 (pd)	XPT1 (nm)	*
RPN12 (pd)	YDR273W (un)	*
RPN5 (pd)	SPC19 (mi)	†
RPN5 (pd)	YDR179C (un)	†
RPN6 (pd)	GCN4 (aa,nm,p2)	*
RPP0 (ps)	RPP1A (ps)	†
RPS26A (ps)	YLR435W (un)	*
RPS26B (ps)	YLR435W (un)	*
RPS28B (ps)	DCP1 (rt)	*
RPS28B (ps)	YBR094W (un)	*
RPS8B (ps)	CKS1 (cc)	*
RPS8B (ps)	GNA1 (cc,wm)	*
RPT3 (pd)	AME1 (ck)	†
RPT3 (pd)	RPT3 (pd)	†
RPT3 (pd)	RPT4 (pd)	†,‡
RPT3 (pd)	RPT5 (pd)	†,‡
RPT3 (pd)	YGR232W (un)	*
RRN10 (p1)	YDL113C (un)	†
RRN7 (p1)	RRN6 (p1)	*,‡
RRN9 (p1)	RRN10 (p1)	*,†¶,‡
RSG1 (un)	YOL083W (un)	*
RTA1 (un)	YHR134W (un)	*
RVS161 (cp,st,mr,vt)	RVS167 (cp,st,vt)	*,*¶,ʃ
RVS161 (cp,st,mr,vt)	YBR108W (un)	*
SAE2 (me)	SAE2 (me)	*
SAE2 (me)	YCR086W (me)	*
SAP4 (cc)	MAD2 (cc,mi)	*
SAP4 (cc)	MAD3 (cc)	*
SAP4 (cc)	PGI1 (cm)	*
SAP4 (cc)	YJL178C (un)	*
SAP4 (cc)	YJL211C (un)	*
SAP4 (cc)	YMR181C (un)	*
SAP4 (cc)	YOR062C (un)	*
SAP4 (cc)	YPR040W (un)	*
SEC14 (li,vt)	YDL001W (un)	*
SEC21 (vt)	YBR281C (un)	*
SED1 (st)	HEM13 (om)	*
SHR3 (pf,sm,vt)	GNP1 (aa,sm)	*
SIN4 (p2)	CDC34 (pd)	*
SIN4 (p2)	CSE1 (mi,nc)	*
SIN4 (p2)	GDS1 (un)	*
SIN4 (p2)	MAD2 (cc,mi)	*
SIN4 (p2)	MAD3 (cc)	*
SIN4 (p2)	PET191 (en)	*
SIN4 (p2)	PRP40 (rp,rs)	*
SIN4 (p2)	QCR6 (en,sm)	*
SIN4 (p2)	YGR046W (un)	*
SIN4 (p2)	YGR117C (un)	*
SIP2 (cm)	SNF4 (si)	*,†¶,ʃ
SKP1 (aa,cc,ch,pd)	BDF1 (ch,me)	†
SKP1 (aa,cc,ch,pd)	CDC4 (cc,pm)	†,*,ʃ
SKP1 (aa,cc,ch,pd)	CTF13 (cc,ch,mi)	†,ʃ
SKP1 (aa,cc,ch,pd)	GRR1 (aa,cm,cc,pd)	†,ʃ
SKP1 (aa,cc,ch,pd)	MET30 (aa,om,pd)	†,ʃ
SKP1 (aa,cc,ch,pd)	RUB1 (cc,pm,ps)	†
SKP1 (aa,cc,ch,pd)	SGT1 (mi,pd)	†,ʃ
SKP1 (aa,cc,ch,pd)	YLR097C (un)	†
SKP1 (aa,cc,ch,pd)	YLR224W (un)	†
SKP1 (aa,cc,ch,pd)	YLR352W (un)	*
SKP1 (aa,cc,ch,pd)	YLR368W (un)	†
SLU7 (rp,rs)	YDL144C (un)	*
SME1 (ch,ds,rp,rs)	SMX3 (ch,ds,rp,rs)	*,‡
SMI1 (wm)	BAS1 (aa,nm,p2)	*
SMK1 (wm,di)	CAK1 (cc,mr,me)	*
SMT3 (pm)	UBC9 (cc,pd,pm)	†,ʃ
SMX3 (ch,ds,rp,rs)	SMD2 (ch,ds,rp,rs)	*
SNF1 (cm,cs,li,si)	GAL83 (cm)	†,*,‡
SNF1 (cm,cs,li,si)	SIP2 (cm)	†,‡
SNF1 (cm,cs,li,si)	YNL218W (ds)	†
SNF4 (si)	COQ5 (en,om)	†
SNF4 (si)	GAL83 (cm)	†,*,‡
SNF4 (si)	YDL214C (un)	†
SNF4 (si)	YJL114W (un)	†
SNF4 (si)	YJR083C (un)	†
SNF4 (si)	YMR291W (un)	†
SNO1 (cs)	SNZ1 (cs)	*,‡
SNO1 (cs)	SNZ3 (cs)	*
SNO3 (cs)	SNZ1 (cs)	*
SNO3 (cs)	SNZ3 (cs)	*
SNP1 (rp,rs)	KIN3 (un)	†
SNU23 (rp,rs)	PRP38 (rs)	*,ʃ
SNZ1 (cs)	SNO1 (cs)	*,‡
SPC19 (mi)	TID3 (mi)	*
SPC34 (ck)	JSN1 (st)	*
SPC34 (ck)	SPC19 (mi)	*
SPO1 (me)	YBR250W (un)	†
SPO11 (me,rc)	SKI8 (rt,rc)	†
SPO12 (di,me)	YCR086W (me)	†
SPO13 (di,me)	ADY1 (un)	*
SPR28 (ck)	CDC11 (cp,wm,ck)	*
SPT2 (ch)	FOB1 (rc)	†
SPT2 (ch)	MCM6 (ds)	†
SRB5 (p2)	MED8 (p2)	*,ʃ
SRB7 (p2)	MED4 (p2)	*
SRB7 (p2)	MED7 (p2)	*
SRL2 (un)	SRL2 (un)	*
SRP1 (cc,nc)	ARG1 (aa,om)	*
SRP1 (cc,nc)	CAR1 (aa,om)	*
SRP1 (cc,nc)	DUT1 (nm)	*
SRP1 (cc,nc)	FCY1 (nm)	*
SRP1 (cc,nc)	ICL1 (cm)	*
SRP1 (cc,nc)	MET17 (aa)	*
SRP1 (cc,nc)	NIF3 (p2,pm)	*
SRP1 (cc,nc)	PHO13 (ph)	*
SRP1 (cc,nc)	SHE2 (cp,di)	*
SRP1 (cc,nc)	SOR1 (cm)	*
SRP1 (cc,nc)	THI6 (om)	*
SRP1 (cc,nc)	TSA1 (cs)	*
SRP1 (cc,nc)	XPT1 (nm)	*
SRP1 (cc,nc)	YAP3 (un)	*
SRP1 (cc,nc)	YFL061W (un)	*
SRP1 (cc,nc)	YGR024C (un)	*
SRP1 (cc,nc)	YMR226C (un)	*
SRP101 (pt)	YMR163C (un)	*
SSP1 (me)	SSP1 (me)	*
STE11 (mr,si)	STE50 (di,mr,si)	*,‡
STE12 (mr,p2,si)	DIG2 (di)	*,ʃ
STE18 (cp,mr,si)	STE4 (mr)	*,‡
STM1 (un)	YJR072C (un)	*
STT4 (li)	GDS1 (un)	*
STT4 (li)	STD1 (cm,cs,sm)	*
SXM1 (nc)	YDR132C (un)	†
SXM1 (nc)	YOL070C (un)	†
SYF1 (rp,rs)	ISY1 (rp,rs)	*,‡
SYF1 (rp,rs)	NTC20 (rp,rs)	*
SYF1 (rp,rs)	SYF2 (rp,rs)	*
SYF3 (rp,rs)	NTC20 (rp,rs)	*
TAF40 (p2)	HMO1 (ch)	*
TAF40 (p2)	TAF25 (p2)	*
TAF60 (p2)	GFD1 (un)	*
TAF60 (p2)	TAF17 (p2)	*,ʃ
TAH18 (un)	GCR2 (p2)	*
TAH18 (un)	GDH2 (aa,om)	*
TAH18 (un)	GDS1 (un)	*
TAH18 (un)	MED1 (un)	*
TEM1 (mi)	DIG1 (di)	†
TEM1 (mi)	DMC1 (me,rc)	†
TEM1 (mi)	ECI1 (li)	†
TEM1 (mi)	FIL1 (en,ps)	†
TEM1 (mi)	FOB1 (rc)	†
TEM1 (mi)	HMO1 (ch)	†
TEM1 (mi)	HSP10 (pf)	†
TEM1 (mi)	KIN3 (un)	†
TEM1 (mi)	LAC1 (vt)	†
TEM1 (mi)	MNS1 (pm)	†
TEM1 (mi)	SEC66 (pt)	†
TEM1 (mi)	SMX3 (ch,ds,rp,rs)	†
TEM1 (mi)	SNZ2 (cs)	†
TEM1 (mi)	SOR1 (cm)	†
TEM1 (mi)	WTM2 (me,p2)	†
TEM1 (mi)	YCR087W (un)	†
TEM1 (mi)	YDL246C (cm)	†
TEM1 (mi)	YEL015W (un)	†
TEM1 (mi)	YHR198C (un)	†
TEM1 (mi)	YJL058C (un)	†
TEM1 (mi)	YJR056C (un)	†
TEM1 (mi)	YLR423C (un)	†
TEM1 (mi)	YNL218W (ds)	†

BD fusion	AD fusion	Source
TEM1 (mi)	YPL192C (un)	†
TFA1 (p2)	TFA2 (p2)	*,∫
TFA1 (p2)	TFB1 (ri,p2)	*
TFB1 (ri,p2)	LAP4 (pd)	*
TFB1 (ri,p2)	SEC35 (vt)	*
TFB1 (ri,p2)	YOL082W (un)	*
THI4 (ri,om)	THI4 (ri,om)	*
THI6 (om)	THI6 (om)	*
TIF35 (ps)	GNA1 (cc,wm)	*
TOP1 (ch,mi)	YMR233W (un)	*
TPK3 (cc)	SRA1 (cc,cs,si)	*,∫
TPK3 (cc)	TPK3 (cc)	†
TPO1 (sm)	CUP2 (cs,p2)	*
TPS2 (cm,cs)	SBH2 (pt)	*
TPS2 (cm,cs)	YAR066W (un)	*
TRS31 (vt)	BET3 (vt)	*,∫
TRS31 (vt)	TRS20 (vt)	*,∫
TRS33 (vt)	YOL082W (un)	*
TSP1 (p2)	YMR316CB (un)	*
UBC6 (pd,pm)	MIR1 (en,sm)	†
UBC6 (pd,pm)	YPL229W (un)	†
UBC9 (cc,pd,pm)	UBC9 (cc,pd,pm)	†
UBP5 (pm)	YBR059C (un)	*
ULA1 (pm)	UBA3 (pm)	*
UME6 (me,om)	GDS1 (un)	*
UME6 (me,om)	YOL082W (un)	*
URA3 (nm)	URA3 (nm)	†
URK1 (nm)	YDR020C (un)	*
VAM7 (mf)	KTR3 (pm)	†
VAM7 (mf)	SEC10 (vt)	†
VAM7 (mf)	SPC72 (me,mi)	†
VAM7 (mf)	STB2 (un)	†
VAM7 (mf)	VAM3 (mf,vt)	†,∫
VAM7 (mf)	YGL104C (sm)	†
VAM7 (mf)	YGL161C (un)	†
VAM7 (mf)	YIF1 (un)	†
VAM7 (mf)	YJL151C (un)	†
VAM7 (mf)	YLR423C (un)	†
VAM7 (mf)	YMR071C (un)	†
VAM7 (mf)	YOL129W (un)	†
VAM7 (mf)	YOR292C (un)	†
VAM7 (mf)	YPL246C (un)	†
VAM7 (mf)	YPT7 (vt)	†
VIK1 (un)	YMR051C (un)	†
VMA22 (ca,sm)	VMA6 (sm)	*
VMA22 (ca,sm)	YDR469W (un)	*
VPS17 (vt)	VPS5 (vt)	*
VPS27 (vt)	YHL002W (un)	*
VPS35 (vt)	CUP2 (cs,p2)	*
VPS36 (vt)	SNF8 (cm,si)	*
VPS4 (vt)	SNF7 (cm,vt)	*
WSC3 (cs,wm)	PEX14 (li,pt)	*
YAL036C (un)	YDR152W (un)	*
YAP5 (p2)	RCS1 (sm)	*
YAR003W (un)	YBR175W (un)	*
YAR003W (un)	YDR140W (un)	*
YAR014C (un)	GLC7 (cm,cs,me,mi)	*
YAR031W (un)	APG12 (pd,pm,vt)	*
YAR031W (un)	YCR030C (un)	*
YBL101W-A (un)	ECM13 (wm)	*
YBL101W-A (un)	URE2 (aa,om,p2)	*
YBL101W-A (un)	YFL002WA (un)	*
YBL101WA (un)	YJL162C (un)	*
YBR006W (un)	RPP2B (ps)	*
YBR006W (un)	YKL023W (rt)	*
YBR052C (un)	YDR032C (un)	*
YBR077C (un)	MVP1 (vt)	*
YBR103W (ch)	YIL112W (un)	*
YBR141C (un)	NBP35 (un)	*
YBR141C (un)	YDR372C (un)	*
YBR190W (un)	SYF3 (rp,rs)	*
YBR228W (un)	YLR135W (un)	*
YBR244W (cs)	SYF3 (rp,rs)	*
YBR270C (un)	GCN3 (ps)	*
YBR270C (un)	TAF17 (p2)	*
YBR270C (un)	YIL105C (un)	*
YCK1 (si)	DUN1 (ri)	†
YCK1 (si)	YER079W (un)	†
YCK1 (si)	YNL116W (un)	†
YCK2 (cp,si)	ADP1 (sm)	*
YCK2 (cp,si)	CTL1 (rp)	*
YCK2 (cp,si)	GDS1 (un)	*
YCK2 (cp,si)	PPA2 (ph)	*
YCK2 (cp,si)	SPB1 (ch)	*
YCK2 (cp,si)	YER079W (un)	*
YCK2 (cp,si)	YKL204W (un)	*
YCL020W (un)	YFL002WA (un)	*
YCL024W (cc)	NAP1 (ch)	*
YCL046W (un)	SNF4 (si)	*,†¶
YCP4 (un)	YDR032C (un)	*
YCR086W (me)	SCM2 (aa,sm)	*
YDL012C (un)	CTH1 (un)	*
YDL012C (un)	GDS1 (un)	*
YDL012C (un)	YFR047C (aa,om)	*
YDL012C (un)	YHR032W (sm)	*
YDL012C (un)	YHR140W (un)	*
YDL012C (un)	YIL172C (cm)	*
YDL012C (un)	YJL065C (un)	*
YDL063C (un)	RPL5 (ps)	*
YDL063C (un)	YRA1 (rp)	*
YDL071C (un)	GNA1 (cc,wm)	*
YDL071C (un)	YDR183W (un)	*
YDL071C (un)	YEL068C (un)	*
YDL071C (un)	YGR269W (un)	*
YDL071C (un)	YNL155W (un)	*
YDL076C (un)	CHA4 (aa)	*
YDL089W (un)	YDL089W (un)	*
YDL089W (un)	YLR324W (un)	*
YDL089W (un)	YMR316CB (un)	*
YDL110C (un)	PUT3 (aa)	*
YDL110C (un)	YOR078W (un)	*
YDL113C (un)	YJL036W (un)	*
YDL133W (un)	YDL001W (un)	*
YDL146W (un)	YKL070W (un)	*
YDL203C (un)	NDD1 (cc,p2)	*
YDL203C (un)	YGR058W (un)	*
YDL213C (un)	YFR032C (un)	†
YDL216C (un)	YMR025W (un)	*
YDL239C (un)	CHA4 (aa)	*
YDL239C (un)	SPO21 (un)	*
YDL239C (un)	SSP1 (me)	*
YDL246C (cm)	SOR1 (cm)	*
YDL246C (cm)	YDL246C (cm)	*
YDR013W (un)	YDR489W (un)	*
YDR026C (un)	FOB1 (rc)	*
YDR032C (un)	STE50 (di,mr,si)	*
YDR032C (un)	YDR032C (un)	*
YDR051C (un)	YDR051C (un)	*
YDR061W (ri)	YCR086W (me)	*
YDR063W (un)	ARC19 (cp,st)	†
YDR063W (un)	YGL239C (un)	†
YDR070C (un)	GNA1 (cc,wm)	*
YDR071C (un)	YBR125C (un)	*
YDR084C (un)	YGL161C (un)	*
YDR084C (un)	YGL198W (un)	*
YDR115W (en,ps)	MRP8 (ps)	*
YDR128W (un)	SEC13 (sm,vt)	*
YDR132C (un)	NMD3 (ca,rt)	*
YDR132C (un)	YJL218W (un)	*
YDR179C (un)	YMR025W (un)	*
YDR200C (un)	FAR3 (cc,mr)	*
YDR200C (un)	YNL127W (un)	*
YDR214W (un)	MAD2 (cc,mi)	*
YDR215C (un)	DBP7 (rp)	*
YDR215C (un)	SPT14 (wm,pm)	*
YDR255C (un)	RPC25 (p3)	*
YDR267C (un)	YHR122W (un)	*
YDR279W (un)	YLR154C (un)	*
YDR326C (un)	YER007CA (un)	*
YDR326C (un)	YIL105C (un)	*
YDR348C (un)	YMR295C (un)	*
YDR357C (un)	SMX3 (ch,ds,rp,rs)	*
YDR400W (un)	YCR059C (un)	*
YDR482C (un)	CAF20 (ps)	*
YDR482C (un)	SCW11 (wm)	*
YEL023C (un)	YDL011C (un)	*
YFR042W (un)	KRE6 (cm,wm)	*
YFR043C (un)	YDR489W (un)	*
YFR047C (aa,om)	YFR047C (aa,om)	*
YGL051W (un)	YAR033W (un)	*
YGL096W (un)	HSH49 (rp,rs)	†
YGL161C (un)	YGL198W (un)	*
YGL198W (un)	YGL161C (un)	*
YGL214W (un)	YLR435W (un)	*
YGL230C (un)	KTI12 (cs)	*
YGL230C (un)	UGA4 (aa,sm)	*
YGL230C (un)	YOR161C (un)	*
YGL242C (un)	BAS1 (aa,nm,p2)	*
YGR010W (un)	YGR010W (un)	*
YGR010W (un)	YLR328W (nm)	*
YGR017W (un)	SFP1 (cc,nc)	*
YGR017W (un)	YLR072W (un)	*
YGR024C (un)	YGR024C (un)	*
YGR058W (un)	HOG1 (cs,si)	*
YGR058W (un)	YGR058W (un)	*
YGR058W (un)	YGR136W (un)	*
YGR058W (un)	YNL047C (un)	*
YGR068C (un)	CKB1 (p3)	*
YGR068C (un)	SFT2 (vt)	*
YGR122W (un)	SNF7 (cm,vt)	*
YGR154C (un)	PWP2 (cp,ck)	*
YGR173W (un)	YDR152W (un)	*
YGR250C (rp)	YIR001C (un)	*
YGR278W (un)	SCM4 (cc)	*
YGR294W (un)	YHL018W (un)	*
YHL002W (un)	VPS27 (vt)	*
YHL002W (un)	YNR005C (un)	*
YHL006C (un)	HDA1 (ch,pm)	*
YHL006C (un)	YDR078C (un)	*
YHL018W (un)	YHL018W (un)	*
YHL046C (un)	GDS1 (un)	*
YHR022C (un)	YIL028W (un)	†
YHR022C (un)	YNR005C (un)	†
YHR039C (un)	DIG2 (di)	*
YHR083W (un)	SPC19 (mi)	†
YHR083W (un)	YNL092W (un)	†
YHR105W (un)	AKR2 (vt)	†
YHR105W (un)	KTR3 (pm)	†
YHR105W (un)	YGL161C (un)	†
YHR105W (un)	YIF1 (un)	†
YHR105W (un)	YPL246C (un)	†
YHR111W (om)	YHR111W (om)	*
YHR115C (un)	YEL041W (un)	†
YHR115C (un)	YLR215C (un)	†
YHR145C (un)	GCN4 (aa,nm,p2)	*
YHR188C (un)	YJR015W (un)	†
YHR197W (un)	YLR423C (un)	†
YHR204W (pm)	RPL30 (ps,rs,rt)	*
YHR204W (pm)	YER126C (un)	*
YIL007C (pd)	ADY1 (un)	*
YIL008W (un)	YHR111W (om)	*
YIL011W (un)	RAD14 (ri)	*
YIL065C (un)	JSN1 (st)	*
YIL065C (un)	SFH1 (ch)	*
YIL074C (un)	YER081W (un)	*
YIL074C (un)	YIL074C (un)	*
YIL082W (un)	YGR024C (un)	*
YIL105C (un)	DMC1 (me,rc)	*
YIL105C (un)	SHE2 (cp,di)	*
YIL105C (un)	YNL047C (un)	*
YIL113W (un)	KNS1 (un)	†
YIL113W (un)	SLT2 (cs,wm,si)	†
YIL132C (un)	SFH1 (ch)	*
YIL132C (un)	YLR322W (un)	*
YIL132C (un)	YLR376C (un)	*
YIL151C (un)	YBL051C (rp)	*
YIL151C (un)	YDR140W (un)	*
YIL151C (un)	YPS4 (un)	*
YIR005W (un)	SPT15 (p1,p2,p3)	†
YIR005W (un)	YGL174W (un)	†,*
YIR005W (un)	YMR057C (un)	†
YJL048C (un)	SHE2 (cp,di)	*
YJL112W (un)	DNM1 (vt)	*
YJL160C (un)	YCR059C (un)	*
YJR024C (cm)	YJR024C (cm)	*
YJR072C (un)	YLR243W (un)	*
YJR072C (un)	YOR262W (un)	*
YJR136C (un)	YKL033W (un)	*
YJU2 (un)	SYF1 (rp,rs)	†
YJU2 (un)	URE2 (aa,om,p2)	†
YKE2 (st)	FAR3 (cc,mr)	*
YKL002W (un)	SPC24 (mi)	*
YKL090W (un)	TBF1 (ch)	*
YKL090W (un)	YGR024C (un)	*
YKL116C (un)	ASK10 (p2,si)	†
YKL116C (un)	STE23 (mr,pm)	†
YKR007W (un)	YBR077C (un)	*
YKR011C (un)	CUP2 (cs,p2)	*
YKR022C (un)	YBL010C (un)	*
YKR022C (un)	YLR424W (un)	*
YKR060W (un)	YDR179C (un)	*
YKR083C (un)	YKL052C (un)	*
YKR096W (un)	YBL051C (rp)	*
YKR104W (sm)	RIB4 (om)	*
YLL049W (un)	YNR069C (un)	*
YLL057C (un)	YLL057C (un)	*
YLL062C (un)	RIB4 (om)	*
YLR015W (un)	YDR469W (un)	*
YLR046C (un)	YHL006C (un)	*
YLR065C (un)	YDL149W (un)	*
YLR215C (un)	YLR386W (un)	*
YLR238W (un)	YDR200C (un)	†
YLR315W (un)	YDR383C (un)	*
YLR328W (nm)	YGR010W (un)	*
YLR328W (nm)	YLR328W (nm)	*
YLR345W (cm)	MTR3 (rp)	*
YLR345W (cm)	SFH1 (ch)	*
YLR368W (un)	IMP2 (pm)	†
YLR368W (un)	TRR2 (cs,om)	†
YLR368W (un)	YHR075C (en,ps)	†
YLR368W (un)	YJL048C (un)	†
YLR368W (un)	YMR048W (un)	†
YLR368W (un)	YPR078C (un)	†
YLR368W (un)	YPR093C (un)	†
YLR392C (un)	JSN1 (st)	*
YLR423C (un)	SEC35 (vt)	*
YLR424W (un)	YKR022C (un)	*
YLR432W (nm)	GCN3 (ps)	*
YLR432W (nm)	GDH2 (aa,om)	*
YLR432W (nm)	TAF25 (p2)	*
YLR432W (nm)	YDR469W (un)	*
YLR465C (un)	AMD1 (nm)	*
YML053C (un)	TDH2 (cm)	*
YML068W (un)	SNF11 (ch,p2)	*
YML088W (un)	SKP1 (aa,cc,ch,pd)	*
YML114C (un)	TAF25 (p2)	*
YML119W (un)	YLL032C (un)	*
YMR025W (un)	POP2 (cm)	*
YMR068W (un)	YIL105C (un)	*
YMR075CA (un)	YCR023C (sm)	*
YMR077C (un)	YKL052C (un)	*

BD fusion	AD fusion	Source
YMR093W (un)	YDR398W (un)	*
YMR102C (un)	YNL218W (ds)	*
YMR210W (un)	MRP8 (ps)	*
YMR269W (un)	GCN3 (ps)	*
YMR312W (un)	IKI1 (un)	*
YMR322C (un)	SNZ1 (cs)	*
YMR322C (un)	SNZ2 (cs)	*
YMR322C (un)	SNZ3 (cs)	*
YNK1 (nm)	YNK1 (nm)	*,∫
YNL201C (cm)	GDS1 (un)	*
YNL201C (cm)	STD1 (cm,cs,sm)	*
YNL201C (cm)	YPR115W (un)	*
YNL218W (ds)	MAD2 (cc,mi)	*
YNL218W (ds)	YNL218W (ds)	*
YNL311C (un)	MET14 (aa,cs,nm,om)	*
YNL311C (un)	YIL074C (un)	*
YNR004W (un)	YPL157W (un)	*
YNR025C (un)	SEC35 (vt)	*
YNR029C (un)	YJL064W (un)	*
YNR029C (un)	YJL065C (un)	*
YNR068C (un)	YNR069C (un)	*
YOL034W (un)	SPC24 (mi)	*,‡
YOL070C (un)	YNL078W (un)	*
YOL106W (un)	SMX3 (ch,ds,rp,rs)	*
YOL111C (un)	SGT2 (un)	*
YOR138C (un)	NPR2 (sm)	*
YOR138C (un)	YGR268C (un)	*
YOR215C (un)	YHR115C (un)	*
YNL056W (un)	SIW14 (cc)	*
YNL056W (un)	YNL099C (un)	*
YNL078W (un)	NAP1 (ch)	*
YNL086W (un)	YKL061W (un)	*
YNL091W (un)	GDS1 (un)	*
YNL091W (un)	YKL075C (un)	*
YNL091W (un)	YNL164C (un)	*
YNL091W (un)	YNL288W (un)	*
YNL091W (un)	YPL229W (un)	*
YOR220W (un)	CUP2 (cs,p2)	*
YOR264W (un)	YCR086W (me)	*
YOR264W (un)	YGR058W (un)	*
YOR353C (un)	NRK1 (wm,mi)	*
YOR353C (un)	SEC35 (vt)	*
YOR353C (un)	YOL082W (un)	*
YPL019C (ca)	VMA22 (ca,sm)	*
YPL110C (un)	YGR024C (un)	*
YPL151C (un)	PEP12 (mf,vt)	*
YPL192C (un)	YPL192C (un)	*
YPL222W (un)	UFD1 (pd)	*
YPL260W (un)	TID3 (mi)	*
YPR105C (un)	PEX14 (li,pt)	*
YPR105C (un)	SEC35 (vt)	*
YPR105C (un)	TIP20 (vt)	*
YPR105C (un)	VMA22 (ca,sm)	*
YPR105C (un)	YLR315W (un)	*
YPR105C (un)	YMR181C (un)	*
YPR105C (un)	YOR164C (un)	*
YNL094W (un)	SSN8 (p2)	*
YNL094W (un)	YAL049C (un)	*
YNL122C (un)	YKL061W (un)	*
YNL127W (un)	RHO4 (cp)	*
YNL127W (un)	TPD3 (cs,p3)	*
YNL157W (un)	ACE2 (p2)	†
YNL157W (un)	YJL075C (un)	†
YNL171C (un)	YCR106W (p2)	*
YNL201C (cm)	AAD6 (mr)	*
YPR105C (un)	YOR331C (un)	*
YPR152C (un)	YBR194W (un)	*
YPT1 (vt)	BOS1 (vt)	†
YPT1 (vt)	KTR3 (pm)	†
YPT1 (vt)	PEP12 (mf,vt)	†
YPT1 (vt)	YPL246C (un)	†
YPT31 (vt)	PEP12 (mf,vt)	†
YPT31 (vt)	YKR030W (un)	†
YPT31 (vt)	YNL146W (un)	†
YPT31 (vt)	YPL192C (un)	†
YPT53 (vt)	SIW14 (cc)	*
YRB1 (nc)	NAP1 (ch)	*
YSC84 (un)	GFD1 (un)	*
YSC84 (un)	SLA1 (cp,st)	*
YSC84 (un)	YGR268C (un)	*
YSC84 (un)	YLR243W (un)	*
YTH1 (rp)	FIP1 (rp)	*,‡
YTH1 (rp)	KTR3 (pm)	*
ZRC1 (cs,sm)	MRP8 (ps)	*

* High throughput screen
† Protein array
‡ Previously known from two-hybrid screens
∫ Previously known to interact or to occur in the same complex as shown by other methods
¶ Found in the other orientation, that is, inverted BD and AD fusions
'Cellular roles' are in parentheses; abbreviations are explained in Table 3.

Table 3 Interactions grouped by protein 'cellular roles' (as classified by the Yeast Protein Database, YPD (ref. 9) [a])

	YPD classification		Results from screens		
	YPD 'cellular roles'	Proteins in category [b]	Proteins identified in both screens [c]	Protein pairs [d]	Protein pairs in category [e]
ag	Ageing	12	0	0	0
aa	Amino-acid metabolism	193	35	71	9
cm	Carbohydrate metabolism	225	38	75	8
ad	Cell adhesion	1	0	0	0
cc	Cell cycle control	136	46	114	17
cp	Cell polarity	81	20	45	4
cs	Cell stress	176	32	61	6
st	Cell structure	79	15	19	4
wm	Cell wall maintenance	152	17	25	1
ch	Chromatin/chromosome structure	174	39	81	9
ck	Cytokinesis	23	6	6	1
di	Differentiation	51	11	42	1
ri	DNA repair	106	20	34	4
ds	DNA synthesis	70	10	24	5
en	Energy generation	237	14	18	1
li	Lipid, fatty-acid and sterol metabolism	161	14	25	3
mr	Mating response	100	24	35	4
me	Meiosis	89	30	65	9
mf	Membrane fusion	23	3	18	1
mt	Mitochondrial transcription	2	1	1	0
mi	Mitosis	107	26	80	4
nc	Nuclear-cytoplasmic transport	75	26	70	9
nm	Nucleotide metabolism	83	20	35	6
ot	Other	11	2	3	0
om	Other metabolism	141	25	46	8
ph	Phosphate metabolism	20	4	14	0
p1	Pol I transcription	27	9	12	3
p2	Pol II transcription	254	65	98	20
p3	Pol III transcription	32	10	18	1
ca	Protein complex assembly	32	5	7	1
pd	Protein degradation	148	36	73	17
pf	Protein folding	53	5	9	0
pm	Protein modification	148	25	42	6
ps	Protein synthesis	338	25	46	7
pt	Protein translocation	77	10	13	3
rc	Recombination	41	13	35	4
rp	RNA processing/modification	252	49	87	32
rs	RNA splicing	102	28	58	24
rt	RNA turnover	28	7	13	0
si	Signal transduction	99	25	61	2
sm	Small molecule transport	373	31	43	3
un	Unknown	2,698	412	509	164
vt	Vesicular transport	229	52	70	15

[a] In the YPD database, proteins have been classified into at least one category, and 32% (1,109) have been placed in more than one category.
[b] Proteins in each category (categ.) based on 6,124 proteins in YPD, of which 3,426 (56%) have a cellular role assigned and 2,698 (44%) are without role assignment.
[c] Total based on the 1,004 proteins identified in the screens.
[d] Protein pairs with at least one protein in the category.
[e] Protein pairs with the two proteins in the same category.